Large Suppression of Quantum Fluctuations of Light from a Single Emitter by an Optical Nanostructure

Diego Martín-Cano,[1,3,*] Harald R. Haakh,[1] Karim Murr,[2,3,4,5] and Mario Agio[2,3,4]
[1]Max Planck Institute for the Science of Light, 91058 Erlangen, Germany
[2]National Institute of Optics (CNR-INO), 50125 Florence, Italy
[3]Center for Quantum Science and Technology in Arcetri (QSTAR), 50125 Florence, Italy
[4]European Laboratory for Nonlinear Spectroscopy (LENS), 50019 Sesto Fiorentino, Italy
[5]Dipartimento di Fisica ed Astronomia, Università di Firenze, 50019 Sesto Fiorentino, Italy
(Received 6 May 2014; revised manuscript received 2 August 2014; published 31 December 2014)

We investigate the reduction of the electromagnetic field fluctuations in resonance fluorescence from a single emitter coupled to an optical nanostructure. We find that such hybrid systems can lead to the creation of squeezed states of light, with quantum fluctuations significantly below the shot-noise level. Moreover, the physical conditions for achieving squeezing are strongly relaxed with respect to an emitter in free space. A high degree of control over squeezed light is feasible both in the far and near fields, opening the pathway to its manipulation and applications on the nanoscale with state-of-the-art setups.

DOI: 10.1103/PhysRevLett.113.263605 PACS numbers: 42.50.Lc, 42.50.Ar, 42.50.Dv, 78.67.-n

Optical nanostructures are known to be efficient architectures for controlling light-matter interactions [1]. Here, near-field effects allow us to modify radiation properties of a broad range of quantum emitters (QEs) covering atoms [2], color centers [3,4], molecules [5,6], or quantum dots [7]. A major goal is now to explore their performance in the quantum regime [8], so far mainly examined in cavity quantum electrodynamics [9]. Antibunching has been investigated as a signature of the granularity of quantum light arising from QEs coupled to nanostructures [3,4,7]. In contrast, electromagnetic field fluctuations below shot noise [10], which mirror the quantum wave nature of light, are known to be challenging to measure [11] at the quantum level and have not been addressed in such hybrid systems.

Reduced quantum fluctuations are the unique characteristics of squeezed states of light [12], which are relevant for overcoming classical application limits in, for instance, precision measurements and spectroscopy. Despite recent experimental [11,13] and theoretical [14,15] advances on the microscopic scale, sources of squeezed light usually rely on the nonlinear response of macroscopic systems, typically crystals or atomic vapors [16].

In this Letter, we show that optical nanostructures can significantly increase squeezing in the resonance fluorescence from a QE. Moreover, they strongly relax the conditions for overcoming shot noise in terms of bandwidth and excitation power. Our results open a pathway towards the experimental measurement of such squeezed states of light in state-of-the-art setups and their manipulation on the nanoscale, with prospects for advancing applications at the single-photon level.

The quantum fluctuations of the electromagnetic field can be measured by homodyne techniques [17]. In the simplest approach, the source field is mixed with a strong coherent field via a beam splitter and collected by a photodetector. This gives access to the variance $(\Delta\hat{\mathcal{E}}_i)^2 = \langle :(\hat{E}_i - \langle\hat{E}_i\rangle)^2: \rangle$ of the electric field quadrature from the source, e.g., the vector component $\hat{E}_i(\mathbf{r},t) = \hat{E}_i^{(+)}(\mathbf{r},t) + \hat{E}_i^{(-)}(\mathbf{r},t)$ along the i direction. Here, we consider normal ordering $(::)$ to directly compare the variance to the shot-noise level, so that negative values of $(\Delta\hat{\mathcal{E}}_i)^2$ indicate squeezed light. We evaluate these fluctuations in the framework of macroscopic quantum electrodynamics in dispersive and absorptive media [17]. In the case of a two-level QE and imposing the rotating wave and Markov approximations, the positive-frequency scattered electric field operator is $\hat{E}_i^{(+)}(\mathbf{r},t) = |g_i(\mathbf{r})|e^{i\phi_i(\mathbf{r})}\hat{\sigma}(t)$, which depends on the QE coherence $\hat{\sigma} = |g\rangle\langle e|$. Here, $|g\rangle$ and $|e\rangle$ are the QE's ground and excited states, respectively. The spatial emission characteristics are encoded in the amplitude $|g_i(\mathbf{r})|$ and phase $\phi_i(\mathbf{r})$, which can be expressed in terms of the classical electromagnetic Green's tensor [18] (see Sec. S1 of the Supplemental Material [19]). Evaluating the fluctuations of $\hat{E}_i(\mathbf{r},t)$, we find

$$[\Delta\hat{\mathcal{E}}_i(\mathbf{r},t)]^2 = 2|g_i(\mathbf{r})|^2[(\langle\hat{\sigma}^\dagger(t)\hat{\sigma}(t)\rangle - |\langle\hat{\sigma}(t)\rangle|^2) - \mathrm{Re}(e^{i2\phi_i(\mathbf{r})}\langle\hat{\sigma}(t)\rangle^2)]. \quad (1)$$

The expectation values are evaluated under steady-state conditions by solving the optical Bloch equations. These contain the effects of the driving field's Rabi frequency Ω, the spontaneous decay rate γ, and the frequency detuning $\delta_L = \omega_L - \omega_E$ between the laser and the QE. We also allow for additional pure dephasing at a rate γ^* [17]. Equation (1) can then be expressed in a form valid for a QE in any environment,

$$[\Delta\hat{\mathcal{E}}_i(\mathbf{r},t)]^2 \underset{\text{steady state}}{=} |g_i(\mathbf{r})|^2 \frac{z^2}{1+\delta^2+z^2} \times \left(1 - \frac{(\delta^2+1)(1+\cos[2\phi_i+2\Phi-2\omega_L t])}{(1+x)(1+\delta^2+z^2)}\right), \quad (2)$$

in terms of the normalized dephasing rate $x = 2\gamma^*/\gamma$, the normalized detuning $\delta = 2\delta_L/(\gamma+2\gamma^*)$, and the normalized Rabi frequency $z = \sqrt{2}|\Omega|/\sqrt{\gamma(\gamma+2\gamma^*)}$. In a homodyne detection scheme, the cosine in Eq. (2) can be set to unity without loss of generality by adjusting the phases ϕ_i and Φ [34]. A detailed derivation of Eqs. (1) and (2) is given in Sec. S2 of the Supplemental Material [19].

From Eq. (1), we see that $(\Delta\hat{\mathcal{E}}_i)^2$ is governed by the QE's optical coherence $\hat{\sigma}$ and upper-state population $\hat{\sigma}^\dagger\hat{\sigma}$ [10]. The fluctuations $\langle\hat{\sigma}^\dagger(t)\hat{\sigma}(t)\rangle - |\langle\hat{\sigma}(t)\rangle|^2$ are always positive, and, hence, tend to destroy squeezing, but they approach zero the weaker the excitation. Since we deal with one QE, a small detection efficiency ($\propto |g_i(\mathbf{r})|^2$ at the detection position) results in low photon count rates, which has prevented the detection of squeezing in free space and made it challenging even in the presence of a cavity [11]. The last term in Eq. (1) originates from quantum fluctuations in the optical coherence $\hat{\sigma}$, which is the only one able to create squeezing. This is a purely nonclassical effect, which is phase dependent and cannot be obtained with coherent light or single photon states [10,12].

If a QE is placed near a nanostructure, the dynamics that generate squeezing are fundamentally changed. First, both the amplitude $|g_i(\mathbf{r})|^2$ and the phase $\phi_i(\mathbf{r})$ are modified by the nanostructure due to its electromagnetic response. Hence, although the field intensity scattered by the QE and consequently the detection efficiency increase [1], its quantum fluctuations can be comparatively reduced with respect to shot noise, with a squeezing amplitude $|g_i(\mathbf{r})|^2$. Second, since $\hat{\sigma}$ is affected by the enhancement of the driving field and the change in γ, both induced by the nanostructure [1], control of these magnitudes can be used to reduce the electromagnetic field fluctuations, while increasing the photon count rate.

For a quantitative analysis, we exemplify the nanostructure with a gold nanosphere (GNS), coupled to a QE characterized by its transition frequency $\omega_E = 2\pi c/\lambda_E$ and dipole $\boldsymbol{d}$, as illustrated in Fig. 1(a). In this case, the Green's tensor $\boldsymbol{G}$ is known analytically. In the far field ($|\mathbf{r}-\mathbf{r}_E| \gg \lambda_E$), $g_i = |g_i|e^{i\phi} \approx (\omega_E^2/\epsilon_0 c^2) G_{ij}(\mathbf{r},\mathbf{r}_E,\omega_E) d_j$ provides an excellent approximation of the amplitude and phase in Eq. (1), whereas a quantum correction must be included in the near field [35] (see Sec. S1 of the Supplemental Material [19]).

Figure 1(b) shows the squeezing amplitude $|g_\theta|^2$ at a detection point in the far field [D_1 in Fig. 1(a)], where the θ component dominates. $|g_\theta|^2$ features several local maxima,

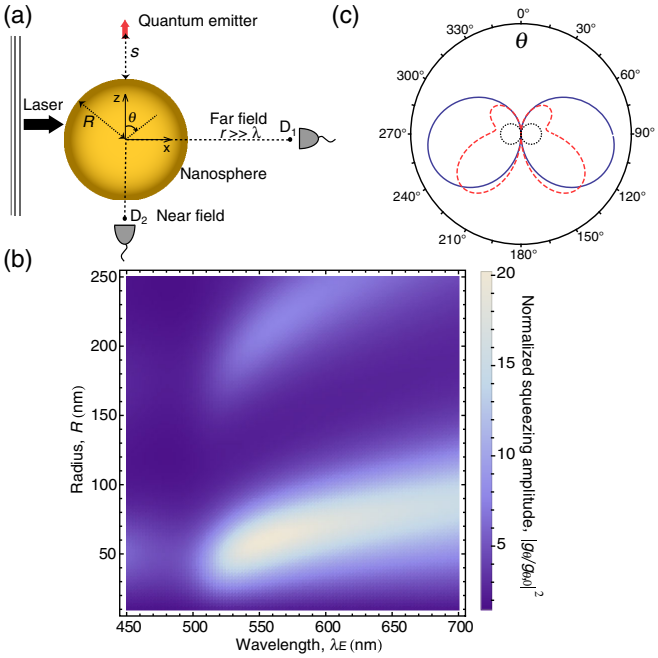

FIG. 1 (color online). (a) A quantum emitter is placed at a distance s from a gold nanosphere of radius R. D_1 and D_2 are detection points in the far and near fields, respectively. D_1 is on the x axis at $10^5\lambda_E$ from the nanosphere center, while D_2 is along the z axis, 10 nm from the nanosphere surface. The emitter dipole moment is perpendicular to the nanosphere surface. (b) Normalized squeezing amplitude $|g_\theta/g_{\theta,0}|^2$ at D_1 as a function of wavelength λ_E and R, for $s = 10$ nm. The θ component of the field quadrature corresponds to the dominant polarization in this configuration. $|g_{\theta,0}|^2$ is the squeezing amplitude in the absence of the nanosphere. (c) Far-field squeezing amplitude $|g_\theta|$, near the dipolar ($R = 60$ nm, solid blue curve) and quadrupolar ($R = 120$ nm, dashed red curve) nanosphere resonances at $\lambda_E = 550$ nm. The dotted black curve corresponds to the free-space case.

arising from the excitation of plasmon-polariton resonances [36], which depend on the GNS radius R and on the QE emission wavelength λ_E. The strongest one originates from the dipole resonance, as indicated by the two-lobe pattern in the far field in Fig. 1(c). Squeezing is enhanced by up to a factor of 20 due to the presence of the GNS. In comparison with a cavity environment, we estimate that the limited mirror transmission leads in fact to a normalized squeezing amplitude slightly lower than the GNS value (see Sec. S3 of the Supplemental Material [19]). The maxima at larger R are associated with higher-order resonances, which reshape the far-field pattern more strongly than the dipolar one [see Fig. 1(c)], yet with a weak dependence on moderate angular variations. Therefore, nanostructures may be exploited to control the directionality of squeezed-state emission in the far field, which can be optimized by suitably designed architectures [37].

The presence of a nanostructure also strongly modifies the conditions for the creation of squeezed light from a QE.

This is possible because $(\Delta\hat{\mathcal{E}}_i)^2$ depends on the frequency detuning δ_L, the Rabi frequency Ω (i.e., the driving field) and the QE's spontaneous decay rate γ, which differ from their values in free space [1] (δ_{L0}, Ω_0, and γ_0, respectively). In practice, the boundaries for the generation of squeezing depend only on the ratios Ω/γ and δ_L/γ [see Eq. (2)]. For a given configuration, these limits are shown in Fig. 2(a) as a function of the rescaled detuning and driving field ($\delta_0 = 2\delta_{L0}/\gamma_0$ and $z_0 = \sqrt{2}\Omega_0/\gamma_0$, respectively). Importantly, we find that the detuning range with sizable squeezing has increased by two orders of magnitude with respect to free space, as displayed in Fig. 2(b). This is directly related to the fact that $\gamma/\gamma_0 \sim 60$ and also to a shift in the resonance frequency. Moreover, squeezing occurs over a much wider range of laser intensities as compared to free space, cf. Fig. 2(b) at zero detuning. The reason is that the GNS has a larger impact on γ than on the field enhancement with respect to free space ($\Omega/\Omega_0 \sim 4.9$ for this case), so that the ratio Ω/γ provides a weaker excitation level at the same incident power ($\propto z_0\Omega/\gamma$).

Realistic QEs can be strongly affected by dephasing [38], which can preclude the generation of squeezing in free space. To gain intuition on how the nanostructure may overcome this difficulty, we show in Fig. 3 $(\Delta\hat{\mathcal{E}}_\theta)^2$ as we vary the distance s [see Fig. 1(a)] at zero detuning, fixed Ω, and assuming an additional rate of pure dephasing, $\gamma^* = \gamma_0/2$. In free space, $(\Delta\hat{\mathcal{E}}_\theta)^2$ exhibits small positive values; i.e., the field fluctuations lie above shot noise. In contrast, the presence of the GNS allows for quantum squeezing over a range of distances that depend on Ω, γ^*, and γ. For example, for $\Omega = 5\gamma_0$, negative values of $(\Delta\hat{\mathcal{E}}_\theta)^2$ occur below $s = 35$ nm and its minimum is reached at $s = 23$ nm. This overall behavior is general, as highlighted by the other curves in Fig. 3 corresponding to a larger Ω. The minimum of each curve results from a nontrivial balance between Ω, γ, the ratio $2\gamma^*/\gamma$, and g_i. All of these depend on the QE position (see the inset of Fig. 3) while Ω is kept constant. Importantly, it is the large increase in γ with respect to the free-space rates γ^* and γ_0 that helps to fulfill the condition set by Eq. (2), cf. [39], but it is in itself not sufficient to warrant squeezing. Still, the condition is robust against the positioning of the QE and squeezing can be achieved over the whole range of distances given in Fig. 3 by adjusting Ω (not displayed). A significant enhancement of the squeezing amplitude is available at distances s of a few tens of nanometers for the considered case. As the QE moves towards the GNS surface, optimal squeezing requires increasingly stronger Ω, especially once s falls below 10 nm, where absorption by real metals provides a dominating nonradiative decay channel for the QE [40]. This is reflected in the growing deviation of γ/γ_0 from $|g_\theta/g_{\theta,0}|^2$ (see inset in Fig. 3). Nevertheless, this figure can be modified by optimized nanostructures [40] and quantum squeezing may, in principle, be enhanced without considerably raising Ω to compensate for the nonradiative losses.

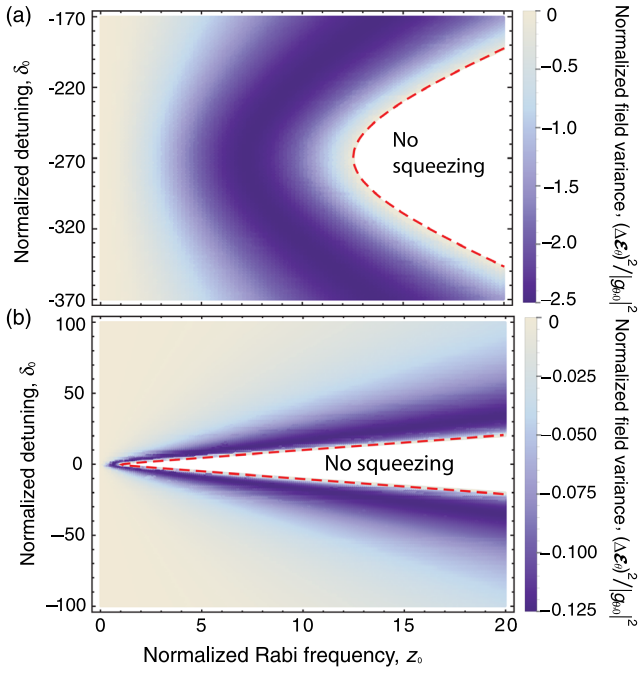

FIG. 2 (color online). Electric field fluctuations with (a) and without gold nanosphere (b). The parameters are $s = 10$ nm, $R = 60$ nm, $\lambda_E = 550$ nm and fields are detected at D_1 [see Fig. 1(a)]. The lower bound of the color scale displays the different minimum value in each panel. Their ratio emphasizes the 20-fold enhancement of squeezing due to the nanosphere as compared to free space.

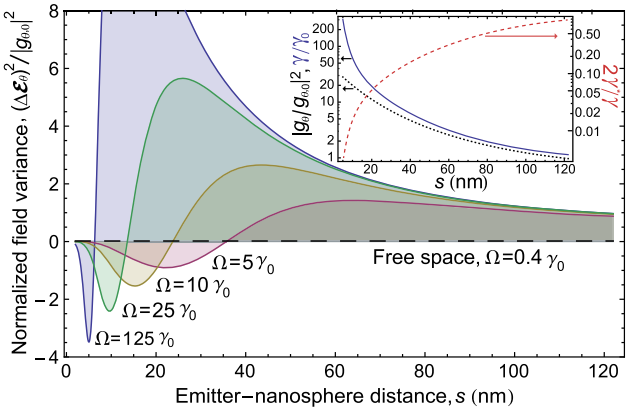

FIG. 3 (color online). Normalized electric field fluctuations as a function of the distance s between the quantum emitter and the nanosphere surface. The quantum emitter is affected additionally by pure dephasing at a rate $\gamma^* = \gamma_0/2$. The curves correspond to different Rabi frequencies Ω. The other parameters are the same as in Fig. 2(a). The result without nanosphere and $\Omega = 0.4\gamma_0$ is represented by a black dashed line. The inset shows the normalized total decay rate γ/γ_0 (solid blue curve) and the field intensity enhancement factor $|g_\theta/g_{\theta,0}|^2$ (dotted black curve) as a function of s. The ratio $2\gamma^*/\gamma$ between the additional pure dephasing and the one associated with spontaneous decay is also displayed (dashed red curve, right axis).

Further enhancement of squeezing can be achieved for detection in the near field, where evanescent modes become relevant. Even in free space, the squeezing amplitude close to a QE is orders of magnitude higher than in the far field, due to the spatial behavior of its dipolar field. To estimate the ability of nanostructures to manipulate squeezed light in the near field, we consider a detection point on the opposite side of the GNS [D_2 in Fig. 1(a)]. Figure 4(a) displays the normalized squeezing amplitude for the radial field component, $|g_r/g_{r,0}|^2$, which dominates in the near-field region. The enhancement leads to values two orders of magnitude larger than those encountered in the far field in the same parameter range of λ_E and R. In contrast with the far field, the enhancement of squeezing increases with higher-order plasmon-polariton resonances at larger R. This arises from the rapid spatial decay of the radial field in free space combined with the field enhancement near the GNS, which boosts the ratio $|g_r/g_{r,0}|^2$. Intuitively, we expect this quantity to increase up to very high R until the system resembles a QE near a flat metal surface, where it becomes limited by propagation losses over the system size [35]. This fact, together with significant experimental evidence

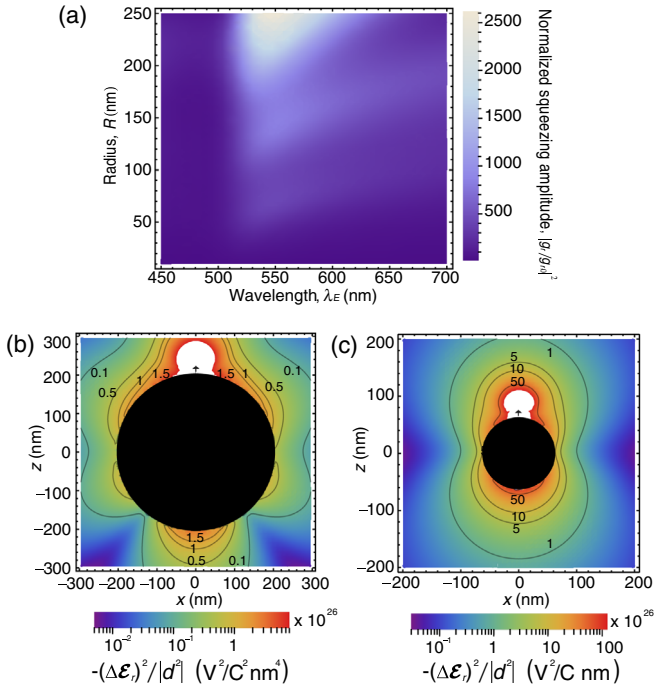

FIG. 4 (color online). (a) Normalized squeezing amplitude for the radial near-field component $|g_r/g_{r,0}|^2$ as a function of λ_E and R, for an emitter-surface distance $s = 10$ nm and detection at D_2 [see Fig. 1(a)]. (b),(c) Contour maps of the negative field fluctuations for the radial component for $R = 200$ nm (b) and $R = 60$ nm (c), with $s = 10$ nm and $\lambda_E = 550$ nm. The values are normalized to the square modulus of the dipole moment $|\mathbf{d}|^2$ to be independent of a specific quantum emitter. The emitter and the nanosphere are represented by a black arrow and a disk in the xz plane, respectively.

[41], suggests that squeezed light generated in such a hybrid system could also be efficiently transferred over a considerable distance by nanoscale waveguides (see Sec. S3 of the Supplemental Material [19]).

For a better understanding of squeezing in the near field, we now analyze the spatial dependence of the electric field fluctuations in proximity of the GNS. Figure 4(b) gives the near-field squeezing pattern for a large GNS ($R = 200$ nm). We observe two lateral lobes, which stem from the excitation of higher-order plasmon-polariton resonances. These are superimposed with the dipolar contribution indicated by the presence of the top and bottom lobes, more clearly visible in Fig. 4(c) in the case of a smaller GNS ($R = 60$ nm). Note that despite the huge enhancements found for large GNSs, the small one improves the squeezing amplitude, e.g., by a factor 30. This is the result of detection closer to the QE combined with a higher near-field enhancement.

Our study indicates a wide range of possibilities for controlling the quantum fluctuations of light at the nanoscale using a laser-driven QE coupled to a nanoarchitecture. We found that the modified dynamics of a QE improve the generation of squeezed light in resonance fluorescence, overcoming the limitations of weak driving. Furthermore, the huge enhancement of spontaneous decay made possible by optical nanostructures [40] may also allow for the generation of squeezed states of light under conditions where the system undergoes fast dephasing. An antenna effect [6] then boosts transfer of squeezing to the far field, resulting in a large suppression of quantum fluctuations. Our results show that the detectable squeezing signal in the electric field quadrature induced by a nanostructure can exceed those achievable in conventional resonators, despite the possibility of a higher inherent QE coherence squeezing of the latter [14,15]. Altogether, these findings facilitate the detection of quantum squeezing in resonance fluorescence from a single emitter within the possibilities of current experiments and provide perspectives for its practical application. Moreover, the large near fields can generate quantum fields on the nanoscale with squeezing levels that are orders of magnitude higher than in the far field. In this regard, future research where QEs and nanostructures are in the strong coupling regime [42] may further advance our understanding on the limits of squeezing at the nanoscale. Our approach may help to develop novel solid-state sources of squeezed light for integrated nanophotonic systems [3,4,7] and quantum-limited sensitivity [16,43], and provide new insights into the production of multipartite entangled states [44,45].

Financial support from the Max Planck Society, the EC Seventh Framework Programme (284584) and the Ministero dell'Istruzione, dell'Università e della Ricerca (2010LLKJBX) are gratefully acknowledged. M. A. wishes to thank Vahid Sandoghdar.

*Corresponding author.
diego-martin.cano@mpl.mpg.de

[1] L. Novotny and N. van Hulst, Nat. Photonics **5**, 83 (2011).
[2] C. Stehle, H. Bender, C. Zimmermann, D. Kern, M. Fleischer, and S. Slama, Nat. Photonics **5**, 494 (2011).
[3] S. Schietinger, M. Barth, T. Aichele, and O. Benson, Nano Lett. **9**, 1694 (2009).
[4] A. Huck, S. Kumar, A. Shakoor, and U. L. Andersen, Phys. Rev. Lett. **106**, 096801 (2011).
[5] P. Anger, P. Bharadwaj, and L. Novotny, Phys. Rev. Lett. **96**, 113002 (2006).
[6] S. Kühn, U. Håkanson, L. Rogobete, and V. Sandoghdar, Phys. Rev. Lett. **97**, 017402 (2006).
[7] A. V. Akimov, A. Mukherjee, C. L. Yu, D. E. Chang, A. S. Zibrov, P. R. Hemmer, H. Park, and M. D. Lukin, Nature (London) **450**, 402 (2007).
[8] M. Tame, K. McEnery, Ş. Özdemir, J. Lee, S. Maier, and M. Kim, Nat. Phys. **9**, 329 (2013).
[9] J.-M. Raimond and S. Haroche, *Exploring the Quantum* (Oxford University Press, Oxford, 2006).
[10] D. F. Walls and P. Zoller, Phys. Rev. Lett. **47**, 709 (1981).
[11] A. Ourjoumtsev, A. Kubanek, M. Koch, C. Sames, P. W. H. Pinkse, G. Rempe, and K. Murr, Nature (London) **474**, 623 (2011).
[12] D. F. Walls, Nature (London) **306**, 141 (1983).
[13] A. H. Safavi-Naeini, S. Groblacher, J. T. Hill, J. Chan, M. Aspelmeyer, and O. Painter, Nature (London) **500**, 185 (2013).
[14] P. Grünwald and W. Vogel, Phys. Rev. Lett. **109**, 013601 (2012).
[15] P. Grünwald and W. Vogel, Phys. Rev. A **88**, 023837 (2013).
[16] R. Loudon and P. L. Knight, J. Mod. Opt. **34**, 709 (1987).
[17] W. Vogel and D.-G. Welsch, *Quantum Optics* (WILEY-VCH, Weinheim, 2006).
[18] C. Tai, *Dyadic Green Functions in Electromagnetic Theory* (IEEE, New York, 1996).
[19] See Supplemental Material at http://link.aps.org/supplemental/10.1103/PhysRevLett.113.263605, which includes Refs. [20–33], for a detailed derivation, a discussion of the homodyne detection scheme, and a comparison to different systems.
[20] L. Knöll, S. Scheel, and D.-G. Welsch, *Coherence and Statistics of Photons and Atoms*, (Wiley, New York, 2001), pp. 1–60.
[21] H. T. Dung, L. Knöll, and D.-G. Welsch, Phys. Rev. A **64**, 013804 (2001).
[22] L.-W. Li, P.-S. Kooi, M.-S. Leong, and T.-S. Yee, IEEE Trans. Microwave Theory Tech. **42**, 2302 (1994).
[23] D. R. Lide, *CRC Handbook of Chemistry and Physics*, 87th ed. (CRC Press, Boca Raton, FL, 2006).
[24] F. Kaminski, V. Sandoghdar, and M. Agio, J. Comput. Theor. Nanosci. **4**, 635 (2007).
[25] D. Dzsotjan, J. Kästel, and M. Fleischhauer, Phys. Rev. B **84**, 075419 (2011).
[26] X.-W. Chen, V. Sandoghdar, and M. Agio, Phys. Rev. Lett. **110**, 153605 (2013).
[27] N. M. Mojarad, V. Sandoghdar, and M. Agio, J. Opt. Soc. Am. B **25**, 651 (2008).
[28] L. Mandel, Phys. Rev. Lett. **49**, 136 (1982).
[29] W. Vogel, Phys. Rev. Lett. **67**, 2450 (1991).
[30] M. Collett, D. Walls, and P. Zoller, Opt. Commun. **52**, 145 (1984).
[31] I. Gerhardt, G. Wrigge, M. Agio, P. Bushev, G. Zumofen, and V. Sandoghdar, Opt. Lett. **32**, 1420 (2007).
[32] M. Agio and V. Sandoghdar, Physica (Amsterdam) **B407**, 4086 (2012).
[33] D. Martín-Cano, L. Martín-Moreno, F. J. García-Vidal, and E. Moreno, Nano Lett. **10**, 3129 (2010).
[34] Besides ϕ_i, the cosine in Eq. (2) contains the phase Φ determined by the driving laser and the coherence operator. Additional phase factors arise in a homodyne scheme for the detection of squeezing and allow for setting the cosine to unity (see Sec. S3 of the Supplemental Material [19]). We impose this condition throughout the numerical evaluations.
[35] H. T. Dung, L. Knöll, and D.-G. Welsch, Phys. Rev. A **65**, 043813 (2002).
[36] C. F. Bohren and D. R. Huffman, *Absorption and Scattering of Light by Small Particles* (John Wiley & Sons, New York, 1983).
[37] A. G. Curto, G. Volpe, T. H. Taminiau, M. P. Kreuzer, R. Quidant, and N. F. van Hulst, Science **329**, 930 (2010).
[38] A. Batalov, C. Zierl, T. Gaebel, P. Neumann, I.-Y. Chan, G. Balasubramanian, P. R. Hemmer, F. Jelezko, and J. Wrachtrup, Phys. Rev. Lett. **100**, 077401 (2008).
[39] The condition for squeezing, i.e., $[\Delta\hat{\mathcal{E}}_i(\mathbf{r},t)]^2 < 0$ in Eq. (2), sets an upper limit for the driving field intensity, $z^2 < (1+\delta^2)(1-x)/(1+x)$. Notice that this requirement cannot be fulfilled for $x \geq 1$, which already occurs for pure dephasing larger that half the spontaneous decay rate.
[40] L. Rogobete, F. Kaminski, M. Agio, and V. Sandoghdar, Opt. Lett. **32**, 1623 (2007).
[41] A. Huck, S. Smolka, P. Lodahl, A. S. Sorensen, A. Boltasseva, J. Janousek, and U. L. Andersen, Phys. Rev. Lett. **102**, 246802 (2009).
[42] A. Trügler and U. Hohenester, Phys. Rev. B **77**, 115403 (2008); J. Bravo-Abad and F. J. Garcia-Vidal, Phys. Rev. Lett. **112**, 253601 (2014).
[43] M. A. Taylor, J. Janousek, V. Daria, J. Knittel, B. Hage, H. A. Bachor, and W. P. Bowen, Nat. Photonics **7**, 229 (2013).
[44] A. Gonzalez-Tudela, D. Martín-Cano, E. Moreno, L. Martín-Moreno, C. Tejedor, and F. J. Garcia-Vidal, Phys. Rev. Lett. **106**, 020501 (2011).
[45] M. Gullans, T. G. Tiecke, D. E. Chang, J. Feist, J. D. Thompson, J. I. Cirac, P. Zoller, and M. D. Lukin, Phys. Rev. Lett. **109**, 235309 (2012).